

26. A. Rahman, M. J. Mandell, J. P. McTague, *ibid.* **64**, 1564 (1976); F. H. Stillinger and T. A. Weber, *ibid.* **80**, 4434 (1984).
27. C. Levinthal, in *Mössbauer Spectroscopy in Biological Systems, Proceedings of a Meeting Held at Allerton House, Monticello, Illinois*, P. DeBrunner, J. Tsubris, E. Munck, Eds. (Univ. of Illinois Press, Urbana, IL, 1969), p. 22.
28. J. D. Bryngelson, J. N. Onuchic, N. D. Socci, P. G. Wolynes, *Proteins* **21**, 167 (1995); P. G. Wolynes, J. N. Onuchic, D. Thirumalai, *Science* **267**, 1619 (1995).
29. M. R. Hoare and P. Pal, *Adv. Phys.* **24**, 645 (1975).
30. B. T. Draine and E. E. Salpeter, *J. Chem. Phys.* **67**, 2230 (1977).
31. D. J. Wales, P. L. A. Popelier, A. J. Stone, *ibid.* **102**, 5556 (1995).
32. P. J. Robinson and K. A. Holbrook, *Unimolecular Reactions* (Wiley-Interscience, London, 1972).
33. H.-P. Cheng and U. Landman, *Science* **260**, 1304 (1993).
34. J. P. Rose and R. S. Berry, *J. Chem. Phys.* **96**, 517 (1992).
35. D. J. Wales, *J. Chem. Soc. Faraday Trans.* **90**, 1061 (1994).
36. We thank T. Astakhova for generating the data base of minima and saddles for the argon cluster. R.S.B. acknowledges the support of the National Science Foundation for this research. R.E.K. acknowledges the support of the Deutsche Forschungsgemeinschaft and the Sonderforschungsbereich 296. A.P. acknowledges the support of the Fulbright Scholar Program. D.J.W. gratefully acknowledges financial support from the Royal Society of London.

10 November 1995; accepted 4 January 1996

Catalytic Cleavage of the C–H and C–C Bonds of Alkanes by Surface Organometallic Chemistry: An EXAFS and IR Characterization of a Zr–H Catalyst

Judith Corker,* Frédéric Lefebvre, Christine Lécuyer, Véronique Dufaud, Françoise Quignard, Agnès Choplin, John Evans, Jean-Marie Basset*

The catalytic cleavage under hydrogen of the C–H and C–C bonds of alkanes with conventional catalysts requires high temperatures. Room-temperature hydrogenolysis of simple alkanes is possible on a well-defined and well-characterized zirconium hydride supported on silica obtained by surface organometallic chemistry. The surface structure resulting from hydrogenolysis of $(\equiv\text{SiO})\text{Zr}(\text{Np})_3$ (Np, neopentyl) was determined from the extended x-ray absorption fine structure (EXAFS) and ^1H and ^{29}Si solid-state nuclear magnetic resonance and infrared (IR) spectra. A mechanism for the formation of $(\equiv\text{SiO})_3\text{Zr-H}$ and $(\equiv\text{SiO})_2\text{SiH}_2$ and the resulting low-temperature hydrogenolysis of alkanes is proposed. The mechanism may have implications for the catalytic formation of methane, ethane, and lower alkanes in natural gas.

The grafting of organometallic compounds onto surfaces is the basis for the rapidly developing field of surface organometallic chemistry. The reactivity of organometallic fragments with surfaces is of special relevance to the understanding of the mechanisms in heterogeneous catalysis, which are still poorly understood, and to the design of well-defined heterogeneous catalysts, which is also a challenge. The potential advantages of catalysts based on surface organometallic fragments over soluble organometallic complexes are considerable: Site isolation prevents undesirable side reactions (notably, bimolecular decomposition pathways), and the problem of catalyst separation and recovery is conveniently resolved. In some cases,

it has been shown that surface organometallic fragments show substantially enhanced reactivity and selectivity compared to analogous molecular complexes or classical heterogeneous catalysts. We report here how the design of a well-characterized zirconium hydride supported on silica can lead to

a solid with remarkable catalytic activity for alkane activation.

The catalytic cleavage of the C–H and C–C bonds of higher alkanes (paraffins) is also a subject of considerable importance. Paraffins are inert materials: Their transformation to lower alkanes (by hydrogenolysis) or to fuels (by dehydrocyclization) usually requires heterogeneous catalysts working at rather high temperatures (typically 500°C). If such reactions could be carried out at a much lower temperature, it would be of great economical advantage. Similar reactions may also play a role in the formation of natural gas (1); it has recently been proposed that ethane and methane may be formed catalytically rather than by thermal decomposition of sedimentary organic matter (1). This hypothesis could alter the way in which we view the generation and distribution of oil and gas in the Earth.

We have discovered that it is possible to carry out the catalytic hydrogenolysis of several simple alkanes (for example, propane, butanes, and pentanes, with the exception of ethane) at mild temperatures by means of a catalyst consisting of a zirconium hydride supported on silica obtained by surface organometallic chemistry (2–6). For example, neopentane (Np-H) was converted into isobutane and methane by the catalyst Zr-H/SiO₂ in the presence of H₂ (1 atm) at 25°C after several hours. If long reaction times (several days) were used, the final products were exclusively methane and ethane (an alkane that is not cleaved by the catalyst under hydrogen). Classical heterogeneous or even homogeneous catalysts and enzymes normally do not achieve under hydrogen such facile cleavage of the C–C bonds of simple alkanes into ethane and methanes (5). We report here the structure of the catalyst and its precursor at an atomic and molecular level. Hereby, we wish to show how this activity can be achieved.

Table 1. The Zr K-edge EXAFS-derived structural parameters for the grafted Zr complexes on silica dehydroxylated at 500°C. For Zr K-edge spectra, AFAC = 0.89* and VPI = -2.0 eV†; values of the photoelectron energy at zero wave vector (E_0) for samples $(\equiv\text{Si-O})\text{ZrNp}_3$ and $(\equiv\text{Si-O})_3\text{ZrH}$ were 13.5 and 20.7 eV, respectively. The Debye-Waller factor is given as $2\sigma^2$, where σ is the root-mean-square internuclear separation. The values given in parentheses represent the statistical errors generated in EXCURVE; for true error estimation, see (6).

Shell	Coordination number	Distance R (Å)	$2\sigma^2$ (Å ²)	R factor (%)
		$(\equiv\text{Si-O})\text{ZrNp}_3$		
O	1.1(1)	1.956(3)	0.0066(8)	29.7
C	3.2(1)	2.219(4)	0.0163(9)	
C	2.8(3)	3.42(1)	0.026(3)	
		$(\equiv\text{Si-O})_3\text{ZrH}$		
O	3.1(1)	1.945(3)	0.0170(5)	27.4
O	1.1(2)	2.61(1)	0.018(3)	

*AFAC, a nondimensional factor describing the effects of multiple excitations resulting in the reduction of EXAFS amplitude, taken to be independent of the environment around the absorbing atom. †VPI, constant imaginary potential describing the lifetime of the photoelectron, describes effects of inelastic scattering in curved wave theory.

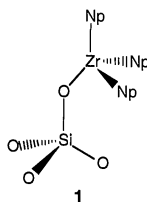
J. Corker and J. Evans, Department of Chemistry, University of Southampton, Southampton SO9 5NH, UK. F. Lefebvre, C. Lécuyer, V. Dufaud, J.-M. Basset, Laboratoire de Chimie Organométallique de Surface, Unité Mixte de Recherche 9986, Centre National de Recherche Scientifique (CNRS)–Ecole Supérieure de Chimie, Physique, et Electronique de Lyon (CPE-Lyon), 69616 Villeurbanne Cedex, France. F. Quignard and A. Choplin, Institut de Recherches sur la Catalyse, CNRS, 69626 Villeurbanne Cedex, France.

*To whom correspondence should be addressed.

Reaction of $ZrNp_4$ with the silanol groups of a Degussa Aerosil silica pretreated at 500°C leads to the surface complex $(\equiv\text{Si}-\text{O})ZrNp_3$ (**1**), which has been characterized previously by surface microanalysis and ^{13}C cross-polarization magic-angle-spinning nuclear magnetic resonance (CP-MAS NMR) and infrared (IR) spectroscopy (2). Treatment of **1** with H_2 at around 150°C leads to the formation of silica-supported zirconium hydride and silicon hydride (**2**) (3–5). We have characterized these various surface species by extended x-ray absorption fine structure (EXAFS) and ^1H and ^{29}Si solid-state NMR and IR spectroscopy.

Analysis of the Zr K-edge EXAFS of **1** (6) (Fig. 1A and Table 1) gave a first coordination sphere of one O atom at 1.96 Å and three C atoms at 2.22 Å; despite the similarity of O and C phase shifts, attempts to fit an O shell at 2.22 Å together with a C shell at 1.96 Å or to fit two shells of O-C resulted in significantly increased refinement (R) factors and unacceptable Debye-Waller factors for the two shells. An additional shell at 3.42 Å could be tentatively assigned to a shell of approximately three nonbonding neopentyl C atoms, although the quality of the data almost certainly limits the precision of this distant shell. The Zr-O distance is similar to those observed in the siloxyzirconium complexes $(\text{DME})ZrCl_2(\text{OSiPh}_3)_2$ [1.91(1) Å] (7) and $[(\eta^5\text{-C}_5\text{H}_5)_2\text{Zr}(\mu\text{-OSiPh}_2\text{O})_2]$ [1.974(2) and 1.983(2) Å] (8) and is also comparable to the Zr-O bond lengths in the hydroxy complexes $\text{Cp}^*_2\text{Zr}(\text{OH})_2$ [1.975(8) and 1.982(7) Å] (9) and $\text{Cp}^*_2\text{Zr}(\text{OH})\text{Cl}$ [1.950(2) Å] (9), suggesting essentially a single-bond charac-

ter in the surface complex (DME, dimethylether; Ph, phenyl; Cp*, pentamethylcyclopentadienyl; the numbers in parentheses after the lengths are the standard errors in the last digits). The Zr-C distance of 2.22 Å is shorter than those observed in $(\eta^5\text{-C}_5\text{H}_5)_2\text{Zr}(\text{CH}_2\text{SiMe}_3)_2$ (Me, methyl) [2.278(4) and 2.281(4) Å] (10), $(\eta^5\text{-C}_5\text{H}_5)_2\text{Zr}(\text{CH}_2\text{CMe}_3)_2$ [2.294(8) Å] (10), and $\text{Zr}(\text{CH}_3\text{Ph})_4$ (2.23, 2.26, 2.28, and 2.29 Å) (11) but is still within the expected range for a Zr-C bond (12). Taking the EXAFS Zr-C and C-C distances as 2.22 and 1.54 Å, respectively, the Zr-C-C angle is calculated to be 130° , with an estimated error of 5° to 10° ; this compares very favorably with the Zr-C-X angles in $(\eta^5\text{-C}_5\text{H}_5)_2\text{Zr}(\text{CH}_2\text{XMe}_3)_2$ (9) of $133.8(2)^\circ$ and $135.2(2)^\circ$ (X = Si) and $142.7(5)^\circ$ (X = C). The EXAFS results thus strongly support the presence of discrete $[\text{Si}]-\text{O}-\text{ZrNp}_3$ surface species.



Treatment of $(\equiv\text{Si}-\text{O})ZrNp_3$ with H_2 at 150°C resulted in a significant change in the Zr K-edge EXAFS (Fig. 1B). This is in agreement with previous in situ IR and NMR experiments, which indicated the formation of a zirconium hydride species (**2**) [zirconium-hydride stretching absorbance $\nu(\text{Zr}-\text{H})$ band at 1635 cm^{-1} and ^1H

MAS NMR peak at chemical shift $\delta = 10$ parts per million (ppm) (3, 13)]. By reaction with various halogenated compounds (such as CH_3I and $\text{C}_2\text{H}_5\text{Br}$), it was found that there is an average of one hydride ligand per Zr (3). Analysis of the EXAFS data revealed a first coordination sphere of three O atoms at 1.94 Å, consistent with single-bond formation. However, the R factor could be decreased by 15% if an additional O at 2.61 Å was included in the EXAFS fit, suggesting a possible longer range Zr interaction with a fourth surface O. These results (EXAFS, IR, NMR, and chemical reactivity) allow us to propose the formulation $(\equiv\text{Si}-\text{O})_3\text{Zr}-\text{H}$ for the supported zirconium hydride species. We suggest a plausible mechanism for its formation (Scheme 1) based on the observation of two IR bands at 2253 and 2195 cm^{-1} , which were attributed to the presence of surface silanes. In addition, the IR data indicate that these surface silanes correspond to a silicon dihydride species (14). The formation of $=\text{SiH}_2$ means that two Si-O bonds of the same Si atom have been broken. The presence of surface silanes has also been indicated by solid-state NMR (13).

The simultaneous formation of $=\text{SiH}_2$ and $(\equiv\text{Si}-\text{O})_3\text{Zr}-\text{H}$ species from the $(\equiv\text{Si}-\text{O})ZrNp_3$ complex demonstrates that the hydrogenolysis of a sterically hindered $(\equiv\text{Si}-\text{O})ZrNp_3$ surface fragment results in the opening of the very strong Si-O-Si bonds. To understand this phenomenon, we must consider a system such as the one depicted in Scheme 1: The postulated ZrH_3 intermediate resulting from the hydrogenolysis of the three neopentyl groups of $(\equiv\text{Si}-\text{O})ZrNp_3$ is bonded to a SiO_4 tetrahedron. We assume that two Si-O-Si bridges of this tetrahedron will be broken, with coordination of the O to the Zr and of the hydride to the Si, in agreement with the above results. Zirconium is more oxophilic than Si and has a similar bonding enthalpy for the M-H bond (M = Zr or Si); therefore, this is a realistic hypothesis. The distance from the O atoms to the Zr atom is not very large (~ 2.4 Å by molecular mechanics), and so the reaction (Scheme 1)

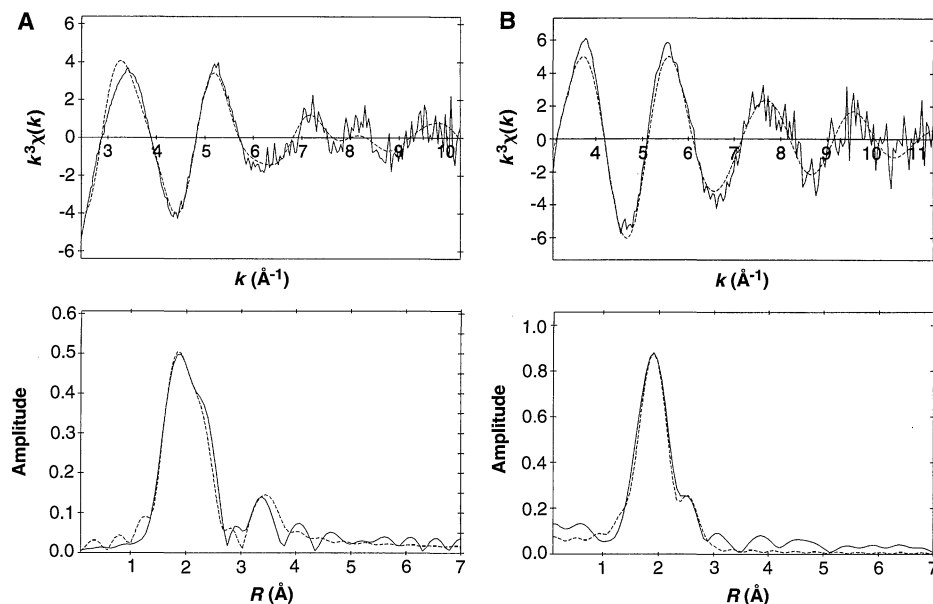
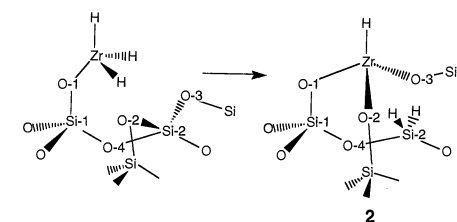


Fig. 1. The (top) Zr K-edge k^3 -weighted EXAFS and (bottom) Fourier transform, phase-shift corrected for oxygen, of (A) $(\equiv\text{Si}-\text{O})ZrNp_3$ and (B) $(\equiv\text{Si}-\text{O})_3\text{-ZrH}$ from experiment (solid lines) and spherical wave theory (dotted lines).

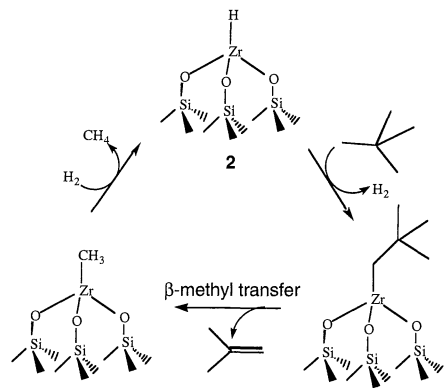


Scheme 1. The Zr, O-1, Si-1, O-4, and Si-2 atoms are shown in the same plane. The atoms O-2 and O-3 are symmetrical with respect to this plane.

should proceed relatively easily. In this model, the =SiH₂ entity is "protected" by the zirconium hydride, probably inducing the long relaxation rates experimentally observed in ²⁹Si NMR (13). Also, the O-4 atom is not very far from the Zr atom (~2.9 Å by molecular mechanics without optimization of the structure); it is probably this O that leads to the EXAFS coordination shell at 2.61 Å. This distance could result from a slight distortion of the SiH₂O₂ tetrahedron (IR data indicate that the H-Si-H angle is ~95°; the O-Si-O angle probably increases compared with its normal value of 109°).

These results show that reaction of the well-defined (≡Si-O)ZrNp₃ complex (where the Zr atom is tetracoordinated) leads to the formation of a zirconium monohydride species, (≡Si-O)₃ZrH, and a silicon dihydride species, =SiH₂. The resulting structure is exceptional and can be interpreted to explain the catalytic process of hydrogenolysis. In this structure, the zirconium hydride has an eight-electron configuration (10 if one considers the O-4 at 2.64 Å). Molecular Zr(IV) hydrides are generally stabilized by two cyclopentadienyl ligands. They are thus 16-electron species and therefore less electrophilic than 2. The immobilization of the hydride on a surface apparently prevents dimerization, which would normally occur for truly molecular species:

We are proposing a mechanism by which the catalyst operates on a "supramolecular" basis, that is, by including both the surface structure of the catalyst and the alkanes. The mechanism is based on preliminary results concerning the elementary steps of C-H bond activation with such a catalyst (3, 4), as well as some elementary steps of β-alkyl transfer that are known to occur when an alkyl group or chain is linked to an early transition metal (15). In the particular case of neopentane hydrogenolysis, the mechanism involves the formation of a Zr-CH₂C(CH₃)₃ species by σ-bond metathesis, followed by β-methyl transfer to give isobutylene and a Zr-CH₃ species. The latter is converted to methane by H₂, with regeneration of the Zr-H catalyst.



The primary product isobutylene was not identified, probably because the catalyst rapidly converted it to isobutane under H₂. Isobutane undergoes further hydrogenolysis to propane and methane; propane is hydrogenolyzed to ethane and methane. Ethane is not cleaved, presumably because the ethylzirconium intermediate lacks a β-methyl group.

This mechanism, which occurs at room temperature, is quite similar to that described by Mango *et al.* (1), which was proposed to explain the methane formation in natural gas. Our results support strongly the assumption that methane in natural gas could be the result of a catalytic process under mild conditions; high temperature may not be a requirement for the formation of natural gas. It is quite possible that under hydrogen [its average concentration in natural gas is ~700 ppm and in some cases can reach 50% (1)], sedimentary rocks containing transition metals such as Zr or Ti may contain a small amount of surface hydride that is able to cleave catalytically the C-H and C-C bonds of alkanes or alkenes.

REFERENCES AND NOTES

- F. D. Mango, J. W. Hightower, A. T. James, *Nature* **368**, 536 (1994).
- F. Quignard *et al.*, *Inorg. Chem.* **31**, 928 (1992).
- F. Quignard, C. Lécuyer, A. Choplin, J.-M. Basset, *J. Chem. Soc. Dalton Trans.* **1994**, 1153 (1994); F. Quignard, C. Lécuyer, A. Choplin, D. Olivier, J.-M. Basset, *J. Mol. Catal.* **74**, 353 (1992).
- F. Quignard, A. Choplin, J.-M. Basset, *Chem. Commun.* **1991**, 1589 (1991).
- C. Lécuyer, F. Quignard, A. Choplin, D. Olivier, J.-M. Basset, *Angew. Chem. Int. Ed. Engl.* **30**, 1660 (1991).
- The x-ray absorption (XAS) spectra were recorded on Station 9.2 of the Synchrotron Radiation Source at the Daresbury Laboratory (2 GeV; average current, ~180 mA) with a Si(220) order-sorting monochromator. Samples for EXAFS analysis were prepared and handled under the strict exclusion of air. XAS cells with Teflon-coated Kapton windows were blown onto break-seal Pyrex tubes containing the silica-supported Zr samples and evacuated to about 0.01 Pa before sample transfer. Spectra were acquired at room temperature in fluorescence mode with a Canberra 13-element solid-state detector. Background-subtracted EXAFS data were obtained with the program PAXAS (16). A polynomial of order 2 was used in the pre-edge background subtraction, and the post-edge background was subtracted by fitting this region with coupled polynomials of order 7 or 8, to remove low-frequency contributions in the spectra. Spherical wave curve fitting analyses, by least squares refinement of non-Fourier filtered EXAFS, were executed in EXCURVE (17), using ab initio phase shifts and backscattering amplitudes calculated from relativistic Hartree-Fock self-consistent-field (HF-SCF)-derived atomic-charge densities. We optimized fits by considering both k^1 and k^3 weightings of the EXAFS because the latter emphasizes the higher shells whereas the former favors near shells or light scatterers. No significant differences were noted for refinements carried out with the two weightings: for the (≡Si-O)ZrNp₃ sample, k^1 -weighted EXAFS refined as 1.3 Zr-O (1.95 Å) and 3.0 Zr-C (2.21 Å), and for the (≡Si-O)₃ZrH sample, 3.2 Zr-O (1.96 Å) and 1.0 Zr-O (2.68 Å). The k^3 -weighted parameters are presented in Table 1. The accuracy of bonded and nonbonded

interatomic distances is considered to be 1.4 and 1.6%, respectively (18). Precisions of first-shell coordination numbers are estimated to be about 5 to 10% and 10 to 20%, respectively. The statistical validity of shells was assessed by published procedures (19), and the numbers of independent parameters used in the fits fall within the guideline $N_{\text{pts}} = 2\Delta k\Delta R / \pi$ (20) (where N_{pts} is the number of independent data points and Δk and ΔR represent the ranges or widths of data in k and R space, respectively, that have been used in the data analysis), unless otherwise stated. The R factor is defined as $(\int |\chi^T - \chi^E| k^3 dk / \int |\chi^E| k^3 dk) \times 100\%$, where χ^T and χ^E are the theoretical and experimental EXAFS and k is the photoelectron wave vector.

- E. A. Babiak, D. C. Hrcir, S. G. Bott, J. L. Atwood, *Inorg. Chem.* **25**, 4818 (1986).
- E. Samuel, J. F. Harrod, M. J. McGlinchey, C. Cabestaing, F. Robert, *ibid.* **33**, 1292 (1994).
- R. Bortolin, V. Patel, I. Munday, N. J. Taylor, A. J. Carty, *Chem. Commun.* **1985**, 456 (1985).
- J. Jeffery *et al.*, *J. Chem. Soc. Dalton Trans.* **1981**, 1593 (1981).
- G. R. Davies, J. A. J. Jarvis, B. T. Kilbourn, A. J. P. Ploli, *Chem. Commun.* **1971**, 677 (1971).
- D. J. Cardin, M. F. Lappert, C. L. Raston, Eds., *Chemistry of Organo-Zirconium and -Hafnium Compounds* (Horwood, Herts, UK, 1986).
- Using ¹H MAS NMR, we detected the zirconium hydride at about 10 ppm as a very unstable species, in agreement with the literature [S. A. Vasnetsov, A. V. Nosov, V. M. Mastikhin, V. A. Zakharov, *J. Mol. Catal.* **53**, 37 (1989)]. Also, the Si and H atoms had very long T_1 relaxation rates (up to 30 s for protons, and more than 200 s for Si atoms). We recorded ²⁹Si CP-MAS NMR spectra after the introduction of O and water on the sample. Peaks corresponding to the Si(OSi)_{4-n}(OH)_n ($n = 0, 1, 2$) entities were observed, together with a broad signal near -70 ppm attributed to Si directly bonded to H. Unfortunately, this does not allow unambiguous differentiation between the ≡SiH and =SiH₂ because the ²⁹Si NMR resonances for these species span the same range (-40 to -80 ppm) [F. C. Schilling, T. W. Weidman, A. M. Joshi, *Macromol. Symp.* **86**, 131 (1994)].
- The two IR bands could correspond to the silicon dihydride species (≡Si-O)₂Si(H)₂ or to the silicon monohydride species (≡Si-O)₃SiH in different environments. The intensity ratio of the two IR bands remains constant for different pretreatment temperatures and silica samples, indicating the formation of the dihydride species. Such formation is also supported by the results from treatment of (≡Si-O)ZrNp₃ with D₂ instead of H₂; in addition to the two bands at 1638 and 1583 cm⁻¹, corresponding to the two Si-D bands at the expected frequency for a SiD₂ species, a peak is detected at 2217 cm⁻¹, as expected for a Si(H)(D) species (the presence of non-negligible amounts of HD in D₂ is probably the result of an exchange reaction of the evolved neopentane). This band cannot be explained if we assume a silicon monohydride species, but can be explained with a very simple harmonic model, if we assume a dihydride species. The frequencies of the two IR bands are given by $\lambda = (\mu_{\text{Si}} + \mu_{\text{H}})(f \pm f')$, where $\lambda = 5.889 \times 10^{-5} \nu^2$, ν is the wave number (in cm⁻¹), μ_{Si} and μ_{H} are 1/28 and 1/1, respectively, and f and f' are the force constant and the interaction constant, respectively. The frequencies of the SiD₂ entity are obtained by replacing μ_{H} (= 1/1) by μ_{D} (= 1/2), yielding 1620 and 1576 cm⁻¹, in reasonable agreement with the experimental frequencies (1638 and 1583 cm⁻¹). For the SiHD species, two IR frequencies are expected at $\lambda = 1/2(B + \Delta^{1/2})$, with $B = 2f(\mu_{\text{Si}} + a)$, $\Delta = 4(\mu_{\text{Si}} + a)^2 f'^2 + (\mu_{\text{H}} - \mu_{\text{D}})^2(f + f')(f - f')$, and $a = 1/2(\mu_{\text{H}} + \mu_{\text{D}})$. The corresponding frequencies are 2223 and 1597 cm⁻¹. The experimentally observed peak at 2217 cm⁻¹ agrees with the first, but the latter frequency is masked by the two SiD₂ bands at 1638 and 1583 cm⁻¹. An H-Si-H angle of 95 ± 5° was estimated from the intensity ratio of the two IR bands, assuming that their respective intensities were proportional to the variation of the dipolar momentum.
- J. J. W. Eshuis, Y. Y. Tan, J. H. Teuben, J. Renkema, J.

- Mol. Catal.* **62**, 277 (1990); J. J. W. Eshuis *et al.*, *Organometallics* **11**, 362 (1992); L. Resconi, F. Piemontesi, G. Francisconi, L. Abis, T. Fiorani, *J. Am. Chem. Soc.* **114**, 1025 (1992); J. Boor, *Ziegler-Natta Catalysts and Polymerizations* (Academic Press, New York, 1979).
16. PAXAS Programme for the Analysis of X-Ray Absorption Spectra; N. Binsted, University of Southampton, Southampton, UK (1988).
17. S. J. Gurman, N. Binsted, I. Ross, *J. Phys. C* **17**, 143 (1984); *ibid.* **19**, 1845 (1986).
18. J. M. Corker and J. Evans, *Chem. Commun.* **1994**, 1027 (1994).
19. R. W. Joyner, K. J. Martin, P. Meehan, *J. Phys. C* **20**, 4005 (1987).
20. F. W. Lytle, D. E. Sayers, E. A. Stern, *Physica B* **158**, 701 (1989).

8 August 1995; accepted 3 November 1995

Lamellar Biogels: Fluid-Membrane-Based Hydrogels Containing Polymer Lipids

Heidi E. Warriner, Stefan H. J. Idziak, Nelle L. Slack, Patrick Davidson,* Cyrus R. Safinya†

A class of lamellar biological hydrogels comprised of fluid membranes of lipids and surfactants with small amounts of low molecular weight poly(ethylene glycol)-derived polymer lipids (PEG-lipids) were studied by x-ray diffraction, polarized light microscopy, and rheometry. In contrast to isotropic hydrogels of polymer networks, these membrane-based birefringent liquid crystalline biogels, labeled $L_{\alpha,g}$, form the gel phase when water is added to the liquid-like lamellar L_{α} phase, which reenters a liquid-like mixed phase upon further dilution. Furthermore, gels with larger water content require less PEG-lipid to remain stable. Although concentrated (~ 50 weight percent) mixtures of free PEG (molecular weight, 5000) and water do not gel, gelation does occur in mixtures containing as little as 0.5 weight percent PEG-lipid. A defining signature of the $L_{\alpha,g}$ regime as it sets in from the fluid lamellar L_{α} phase is the proliferation of layer-dislocation-type defects, which are stabilized by the segregation of PEG-lipids to the defect regions of high membrane curvature that connect the membranes.

Gels are viscoelastic materials that normally consist of a solid component dispersed in a liquid, water in the case of hydrogels. Polymer gels (1)—either natural, such as gelatin, or synthetic—contain a polymer network (2), which serves as the solid component and can resist shear. For many biological applications, gels based on high molecular weight poly(ethylene oxide) [PEO, $(\text{OCH}_2\text{CH}_2)_n$] (3) have been used because of their low immunogenicity: the material can be used to coat more immunogenic tissues (1) and materials (4).

Recent studies show that attaching low molecular weight ($n < 150$) PEO (referred to as PEG) to a biological macromolecule (5–8) can dramatically increase blood circulation times. Both peptides and proteins can be protected by covalently attached PEG for in vivo administration of therapeutic enzymes (5), and so-called “Stealth” liposomes (6–8) consisting of closed bilayer shells of phospholipids covered with PEG-lipids hydrophobically anchored to the membrane can be used as a drug carrier system. The inhibition of the body’s im-

mune response to these PEG-coated liposomes has been attributed (8) to a polymer-brush-type steric repulsion (9) that has been measured between PEG-coated membranes incorporated both in the chain-frozen membrane phase on a solid substrate (10) and in the chain-melted fluid phase in multilamellar L_{α} systems (11). In these systems, the emphasis was in the regime where the intermembrane distance $d \leq R_g$, where R_g is the PEG radius of gyration.

In exploring the interactions between PEG-lipid and the chain-melted fluid phase in multilamellar L_{α} systems, we have discovered a lamellar hydrogel phase, labeled $L_{\alpha,g}$, in the high water regime of the phase diagram. This gel incorporates no solid phase component. Polarized light microscopy has revealed that this phase is not isotropic and shows liquid crystal-like birefringence. Studies with x-ray diffraction show that the maximum interlayer spacings $d \gg R_g$ for this phase (Fig. 1A); a model for the structure of this phase suggests that PEG-lipid stabilizes layer dislocation defects in regions of high membrane curvature (Fig. 1B). Unlike L_{β} gels that incorporate solid membranes (12), a bioactive gel based on fluid membranes could incorporate membrane-embedded proteins that are biologically active, thus providing a way in which to deliver such molecules in a stable gel. An unusual feature of these gels is that they can be formed from a liquid-like flowing L_{α}

phase by adding water and also dissolved back to a flowing two-phase liquid by further addition of water.

The $L_{\alpha,g}$ phase is composed of membranes of DMPC (dimyristoyl phosphatidyl choline), the co-surfactant pentanol, and small amounts of the polymer-lipid PEG-DMPE {1,2-diacyl-*sn*-glycero-3-phosphoethanolamine-*N*-[poly(ethylene glycol)]} separated by water. The PEG-lipid is hydrophobically anchored but free to diffuse within the fluid membrane (Fig. 1A). We investigated two different molecular weights of PEG, 2053 g/mol (PEG2000; $n = 45$ monomers) and 5181 g/mol (PEG5000; $n = 113$) (Avanti Polar Lipids, Alabaster, Alabama). The most dilute gels contained 90.0 weight % water, 6.0 weight % lipid, 3.46 weight % pentanol, and 0.54 weight % PEG5000-DMPE (Fig. 2). In contrast, the conventional solid-membrane L_{β} gels incorporate at most 40 weight % water (12). In principle, addition of PEG-lipid to even more dilute L_{α} phases [≈ 99 weight % (13)] would result in extremely dilute lamellar gels.

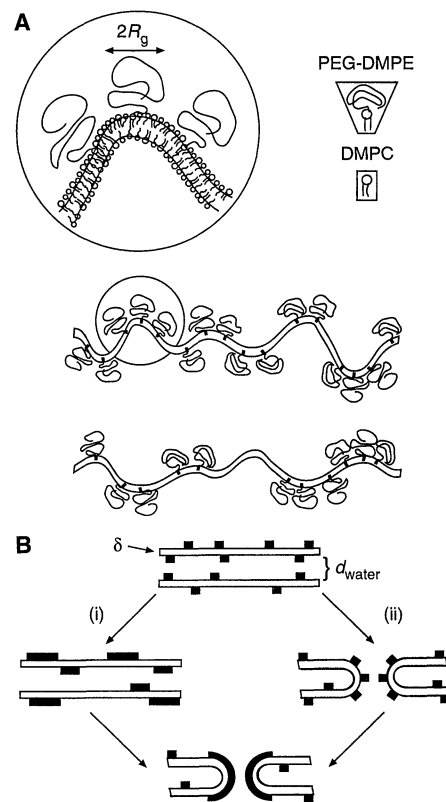


Fig. 1. (A) Schematic of two undulating fluid membranes [composed of DMPC and co-surfactant pentanol (single chain)] with PEG-lipid hydrophobically anchored but freely diffusing within the membrane. (B) Schematic of two paths that would form defects, with the laterally phase separated PEG-lipid residing in, and stabilizing, the regions of high curvature. The interlayer spacing is $d = \delta + d_{\text{water}}$, where δ is the membrane thickness and d_{water} is the separation between layers containing water and the hydrophilic PEG component.

Materials Research Laboratory, Materials Department, Physics Department, and the Interdepartmental Biochemistry and Molecular Biology Program, University of California, Santa Barbara, CA 93106, USA.

*Permanent address: Laboratoire de Physique des Solides (CNRS), Bat. 510, Université Paris Sud, 91405 Orsay, Cedex, France.

†To whom correspondence should be addressed.